

Mass spectrometric *N*-glycan analysis of haptoglobin from patient serum samples using a 96-well plate format

Jianhui Zhu¹, Jing Wu¹, Haidi Yin¹, Jorge Marrero², and David M. Lubman^{1}*

¹Department of Surgery, University of Michigan Medical Center, Ann Arbor, MI 48109

²UT Southwestern Medical Center, Department of Internal Medicine, Dallas, TX 75390

Supporting Information

Table of Contents

Figure S1. HPLC chromatogram of a human haptoglobin standard

Figure S2. HPLC chromatogram of haptoglobin enrichment from patient serum and 1D gel analysis

Figure S3. Comparison between HPLC platform versus IP method for serum Hp enrichment

Figure S4. MALDI-QIT-TOF MS/MS spectra for glycan composition assignment

Figure S5. MALDI MS spectra of *N*-glycans from sequential aliquots of a human haptoglobin standard

Figure S6. MALDI MS analysis of four replicates of haptoglobin derived from an HCC patient serum

Table S1. The binding efficiency of the anti-Hp HPLC column measured by a human Hp standard

Table S2. Eight *N*-glycans identified in serum haptoglobin after desialylation and permethylation

Table S3. The bifucosylation and core-fucosylation degrees of Hp in individual serum samples

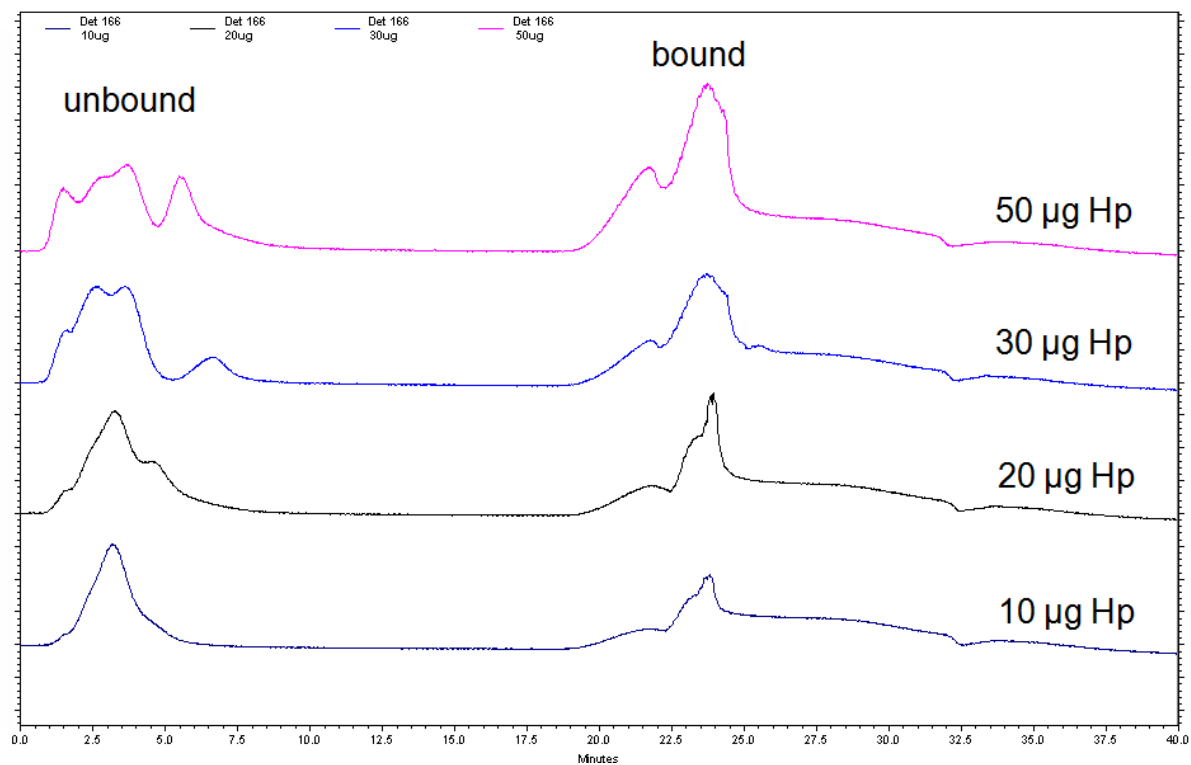


Figure S1. The chromatogram shows the binding efficiency of the antibody-immobilized HPLC column which was measured by a human haptoglobin standard with different loading amounts, i.e. 10, 20, 30, and 50 µg, respectively.

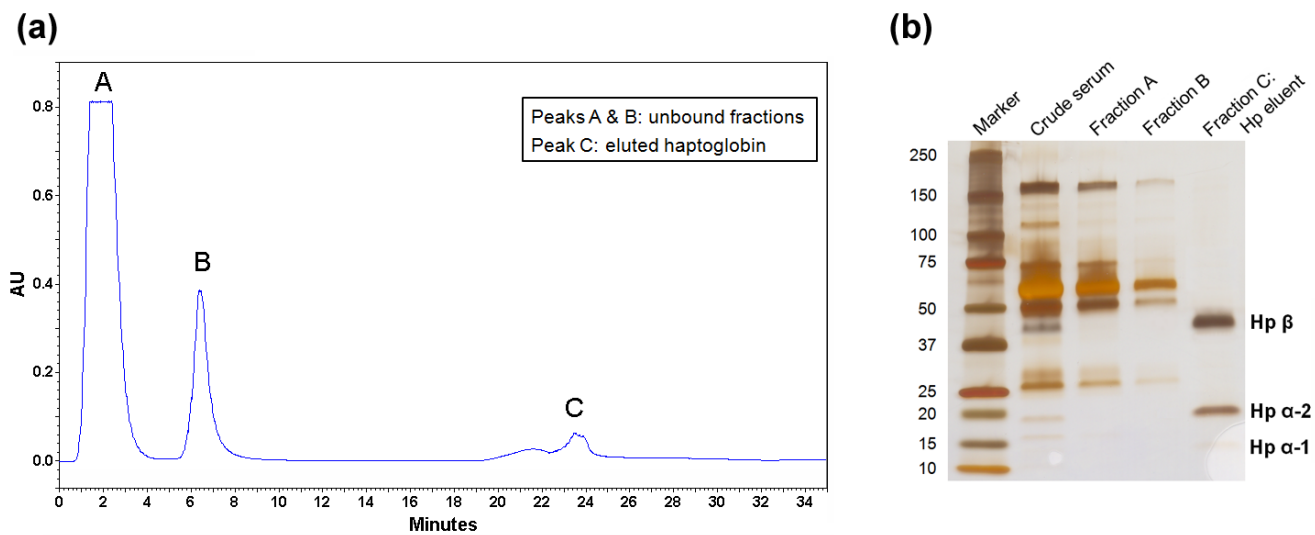


Figure S2. (a) A representative chromatogram of haptoglobin enrichment from patient serum using an antibody-immobilized HPLC platform. (b) 1D gel analysis of unbound fractions A and B, and the eluted fraction C after HPLC enrichment. 1/400 of fraction A and B, and 1/10 of haptoglobin eluent, as well as crude serum (0.1 μ L) were run on a 4–20% SDS-PAGE gel and visualized by silver staining using ProteoSilver™ Plus Silver Stain Kit (Sigma).

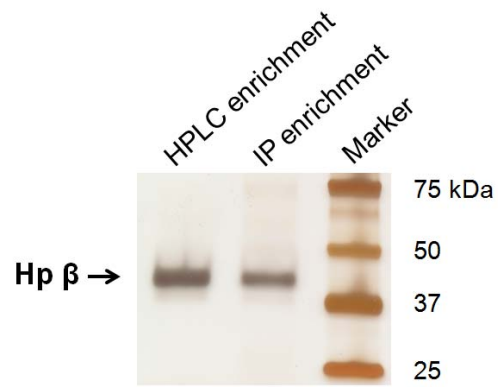


Figure S3. Comparison of the yield of haptoglobin enriched from patient serum using the antibody-immobilized HPLC platform versus the conventional immunoprecipitation method. One-tenth of the haptoglobin eluent from the HPLC column and immunoprecipitation, respectively, were run on a 4–20% SDS-PAGE gel and visualized by silver staining.

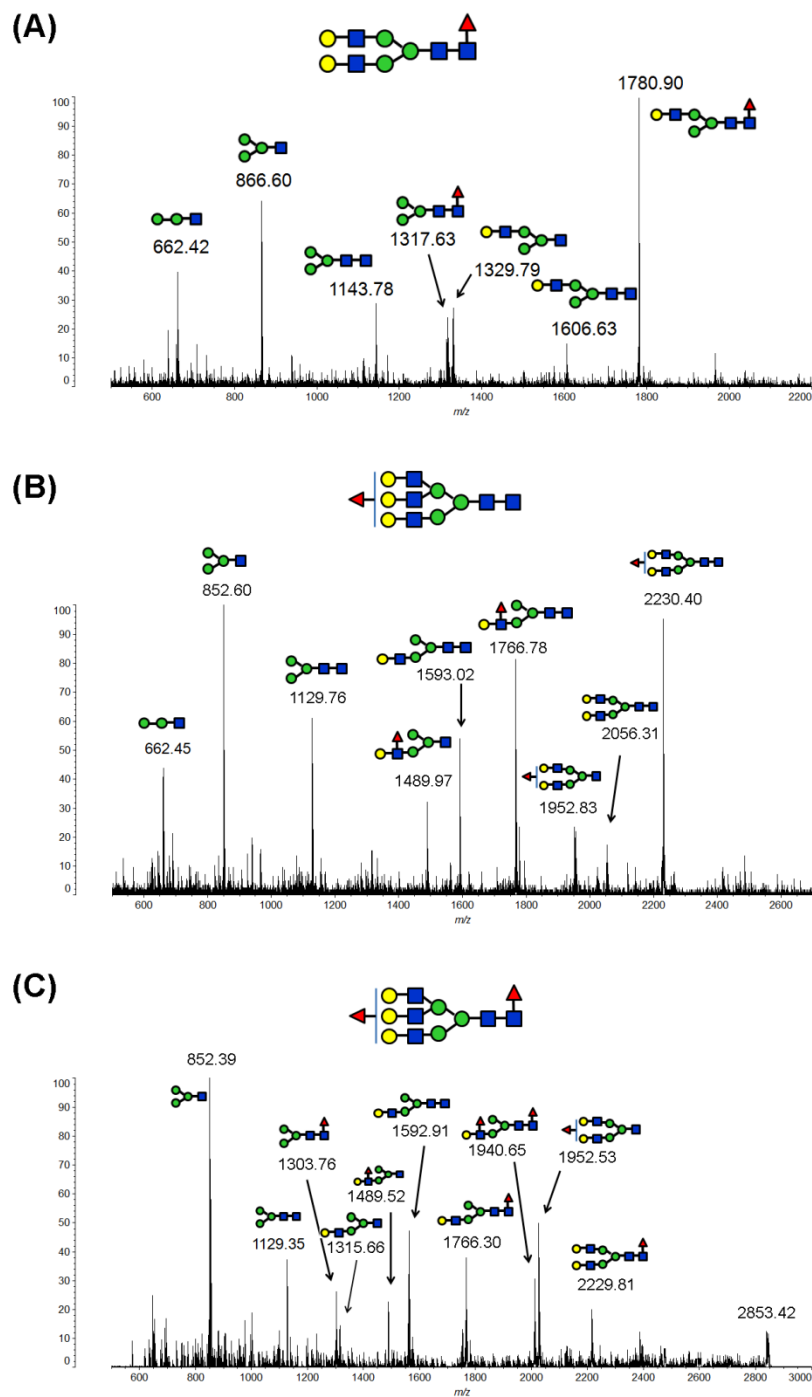


Figure S4. Representative MALDI-QIT-TOF MS/MS spectra of glycans at (A) m/z 2244.13, (B) m/z 2693.40, and (C) m/z 2867.48 for glycan composition and core/antennary fucosylation assignment. Potential structures of fragment ions are labeled. At low energy CID, the predominant fragments are y -ions resulting from the cleavage of labile GlcNAc-Hex glycosidic bond; therefore, the oligosaccharide composition can be inferred from mass differences of fragment ions. (A) The fucosylated biantennary glycan (m/z 2244.13) is confirmed as core fucosylated because of a diagnostic fragment at 1317.63

which corresponds to a fucosylated pentasaccharide core. This conclusion is also supported by an ion at 1329.79 resulting from loss of core Fuc-GlcNAc. (B) The fucosylated tri-antennary glycan (m/z 2693.40) is confirmed as antennary fucosylated. A diagnostic peak at m/z 1952.83 is the cleavage product of peak at 2230.40 after loss of core GlcNAc, indicating that there is no core fucose attached originally. (C) The bifucosylated triantennary glycan (m/z 2867.48) is determined as a triantennary structure with both core and antennary fucosylation. The fragment ion at m/z 1940.65 is the product after loss of two nonreducing terminal Gal-GlcNAc residues, with two attached fucose residues. Core fucosylation is confirmed by the presence of a fragment ion at m/z 1303.76 corresponding to a fucosylated pentasaccharide core structure. A peak at m/z 1489.52 resulting from loss of core Fuc-GlcNAc unambiguously indicates antennary fucosylation.

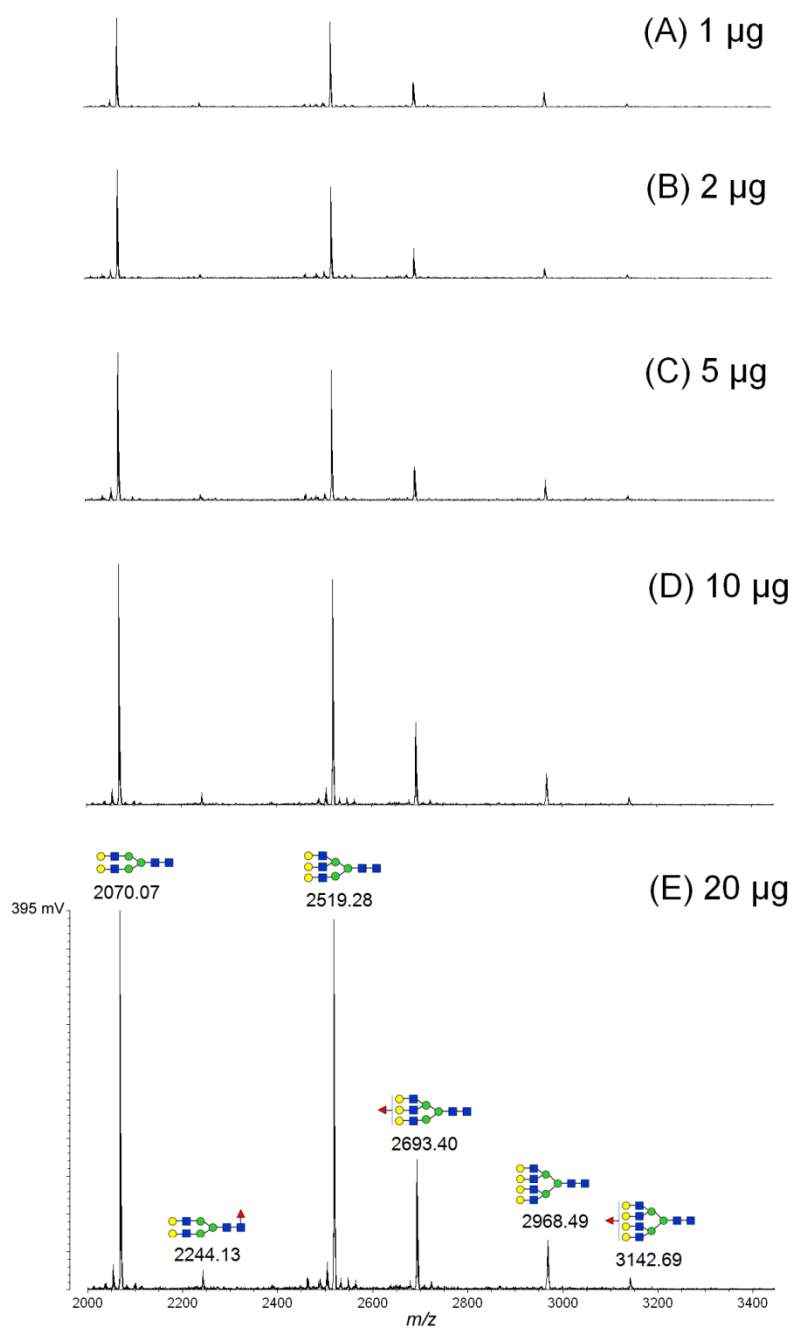
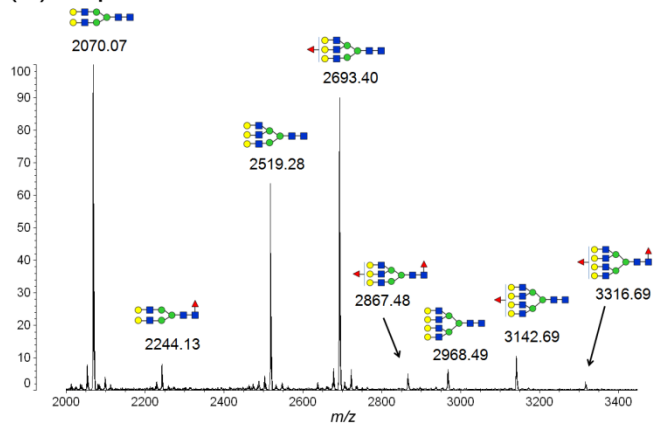
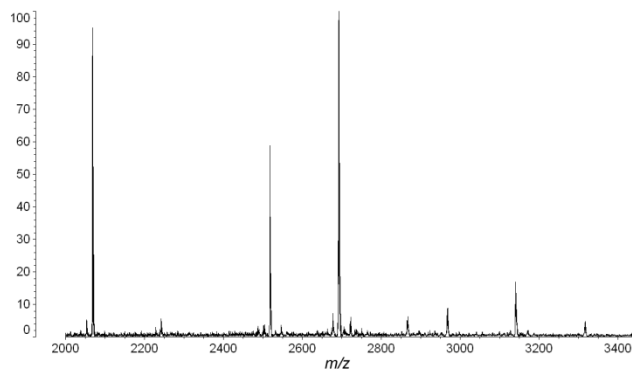


Figure S5. MALDI-QIT-TOF MS spectra of *N*-glycans from a human haptoglobin standard processed on the 96-well plate format in sequential aliquots of 1, 2, 5, 10, and 20 μg , respectively.

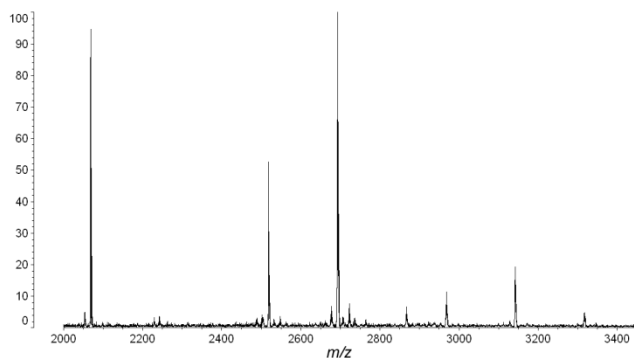
(A) Replicate 1



(B) Replicate 2



(C) Replicate 3



(D) Replicate 4

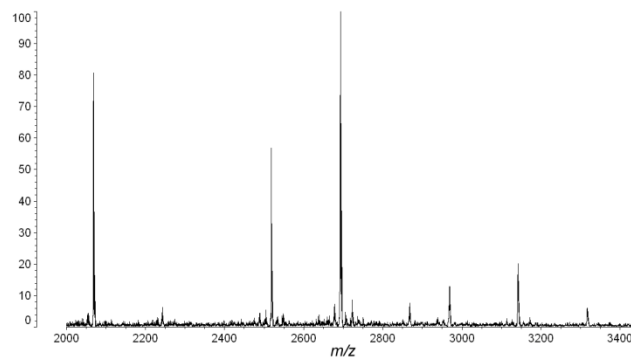


Figure S6. MALDI-QIT-TOF MS analysis of four replicates of haptoglobin derived from 10 μ L of serum of an ALC-related HCC patient followed by *N*-glycan processing on the 96-well plate format.

Table S1. The binding efficiency of the anti-Hp HPLC column measured by a human haptoglobin standard, which was calculated by the ratio of peak area of the bound fraction to the sum of peak areas of bound and unbound fractions.

Loading amount (Hp)	Peak area of unbound fraction	Peak area of bound fraction	Binding efficiency
10 μ g	3601794	6995444	66.0%
20 μ g	5201635	8175367	61.1%
30 μ g	5701265	9495381	62.5%
50 μ g	6980786	12480825	64.1%

Table S2. Eight *N*-glycans identified in serum haptoglobin after desialylation and permethylation.

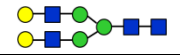

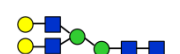



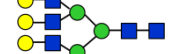

Peak No.	Observed <i>m/z</i>	Calculated <i>m/z</i>	Glycan structure
1	2070.07	2070.03	
2	2244.13	2244.12	
3	2519.28	2519.26	
4	2693.40	2693.35	
5	2867.48	2867.44	
6	2968.49	2968.49	
7	3142.69	3142.58	
8	3316.69	3316.67	

Table S3. The bifucosylation and core-fucosylation degrees of haptoglobin enriched from individual serum samples including 15 HCC and 15 cirrhosis cases.

Sample No.	Bifucosylation degree		Core-fucosylation degree	
	HCC	Cirrhosis	HCC	Cirrhosis
1	0.0989	0.0268	0.1782	0.0986
2	0.0871	0.0252	0.1685	0.0962
3	0.1060	0.0389	0.1811	0.1582
4	0.0554	0.0159	0.1217	0.0793
5	0.0770	0.0139	0.1563	0.0837
6	0.0964	0.0233	0.1149	0.1830
7	0.0982	0.0384	0.1628	0.1307
8	0.1174	0.0317	0.2535	0.1278
9	0.0755	0.0384	0.1472	0.1307
10	0.0649	0.0069	0.1379	0.0944
11	0.0589	0.0329	0.1207	0.1493
12	0.0688	0.0281	0.1378	0.1098
13	0.0634	0.0287	0.1318	0.1188
14	0.0807	0.0430	0.1565	0.1603
15	0.0729	0.0344	0.1351	0.1653
Mean \pm SD	0.081 \pm 0.018	0.028 \pm 0.010	0.15 \pm 0.0089	0.13 \pm 0.0083